

Drought-induced discontinuities in the source and degradation of dissolved organic matter in a Mediterranean river

Joan P. Casas-Ruiz  · Jörg Tittel · Daniel von Schiller · Núria Catalán · Biel Obrador · Lluís Gómez-Gener · Elke Zwirnmann · Sergi Sabater · Rafael Marcé

Received: 13 June 2015 / Accepted: 11 December 2015 / Published online: 23 December 2015
© Springer International Publishing Switzerland 2015

Abstract The composition of dissolved organic matter (DOM) in rivers results from the different sources and in-stream transformations along the land to ocean aquatic continuum. Riverine DOM sources are highly dependent on the hydrological connection between the river channel and the surrounding terrestrial ecosystems, but how the lack of this connectivity (e.g., during drought episodes) affects the sources and biodegradation of DOM in rivers remains unclear. Here we identified the DOM sources as well as the

different DOM pools that are respired along a Mediterranean river during drought by combining absorbance-fluorescence spectroscopy, size-exclusion chromatography, biodegradation assays, and stable and radiocarbon isotopes. DOM composition was highly heterogeneous along the river in response to different sources and in-stream processes in each distinct aquatic environment (i.e., isolated water pools, running waters, and impounded waters in weirs). The reduced hydrological connectivity with terrestrial ecosystems promoted the influence of autochthonous DOM sources. Still, tree leaves from

Responsible Editor: J. M. Melack.

J. P. Casas-Ruiz (✉) · S. Sabater · R. Marcé
Catalan Institute for Water Research (ICRA), Emili Grahit
101, 17003 Girona, Spain
e-mail: jpcasas@icra.cat

J. Tittel
Department Lake Research, UFZ Helmholtz Centre for
Environmental Research, Brückstr. 3a, 39114 Magdeburg,
Germany

D. von Schiller
Department of Plant Biology and Ecology, Faculty of
Science and Technology, University of the Basque
Country, Apdo. 644, 48080 Bilbao, Spain

N. Catalán
Department of Ecology and Genetics/Limnology,
Evolutionary Biology Centre, Uppsala University,
Norbyvägen 18D, 75236 Uppsala, Sweden

B. Obrador · L. Gómez-Gener
Department of Ecology, University of Barcelona, Av
Diagonal 643, 08028 Barcelona, Spain

E. Zwirnmann
Leibniz-Institute of Freshwater Ecology and Inland
Fisheries, Müggelseedamm 301, 12587 Berlin, Germany

S. Sabater
Institute of Aquatic Ecology, University of Girona,
17071 Girona, Spain

overhanging canopies stood out as an important terrestrial DOM source, especially in sites where water residence time was high such as isolated pools and weirs. Degradation of leaf leachates was a relevant process in these sites, whereas autochthonous DOM and groundwater millennial DOM (>1300 year B.P.) seemed to be degraded in running waters. Overall, our results highlight that the drought-induced hydrological disconnection entails a great spatial heterogeneity in the sources of DOM, which at the same time determines the different DOM pools that are respired in each environment along the river.

Keywords Mediterranean rivers · Drought · Dissolved organic matter · Degradation · Radiocarbon

Introduction

Dissolved organic matter (DOM) is the major pool of reduced carbon (C) in transport from the continents to the ocean (Volk et al. 1997) and represents the primary substrate for microbial communities in freshwaters (Benner 2003). The amount and composition of DOM in rivers is the combined result of its different sources and in-stream transformation processes such as biodegradation, photodegradation, or flocculation (Aitkenhead-Peterson et al. 2003; Sinsabaugh and Foreman 2003; Sachse et al. 2005). Depending on its source, DOM can be classified either as autochthonous, when produced within the aquatic system itself, or allochthonous when it derives from terrestrial ecosystems. Autochthonous DOM is generally assumed to be rich in biologically reactive components due to its inherent properties (e.g. low molecular weight, high nitrogen content; Bertilsson and Jones 2003), whereas terrestrial DOM has been traditionally considered as an heterogeneous mixture of contemporary and aged compounds (Raymond and Bauer 2001; Butman et al. 2012) that is recalcitrant and contributes little to freshwater ecosystem metabolism (Wetzel 1983). However, the high prevalence of net heterotrophy and carbon dioxide (CO₂) supersaturation in freshwaters implies that terrestrially derived C is significantly contributing to ecosystem respiration (Cole and Caraco 2001; Duarte and Prairie 2005; Battin et al. 2008) and subsidizing river food webs (Caraco et al. 2010), even if this C is ancient

(McCallister and Del Giorgio 2012; Fellman et al. 2015). Therefore, a comprehensive accounting not only of the sources but also the biodegradability of DOM is paramount to elucidate the role of river networks on the continental C cycle (Cole et al. 2007; Battin et al. 2008).

Because most riverine DOM originates from terrestrial ecosystems (Wetzel 1983; Cole and Caraco 2001), its specific sources are highly dependent on the hydrological connection between the river channel and both the riparian and groundwater systems (Aitkenhead-Peterson et al. 2003). Nevertheless, how the lack of hydrological connectivity affects the sources and biodegradation of DOM in rivers has been rarely explored. This situation often takes place in arid and semiarid regions, where river networks are subject to a dynamic hydrological regime that usually involves drought episodes (Gasith and Resh 1999). During these periods, lowering water tables reduce the hydrological connectivity between the river and its catchment as well as along the river flow path (i.e. longitudinal fragmentation; Bernal et al. 2013). In addition, such loss of connectivity is enhanced by a myriad of man-made flow discontinuities such as weirs and impoundments, which are widespread in these regions (Döll et al. 2009). In this sense, drought turns river networks into a fragmented and heterogeneous landscape dominated by slow running waters, isolated water pools and weirs, where the hydrological connectivity with terrestrial ecosystems is reduced to deeper groundwater inputs (Dahm et al. 2003).

During drought, the prevalence of more autochthonous DOM has been reported in semiarid temporary streams in comparison to other hydrological situations (Vazquez et al. 2011; Ylla et al. 2011; von Schiller et al. 2015). Particularly, the last stages of drought when the river network can be highly fragmented have been described as hot moments of autochthonous DOM production (von Schiller et al. 2015; Vazquez et al. 2015). Recent findings also highlight great spatial heterogeneity in the quantity and composition of the riverine DOM during these periods, with isolated pools standing out as distinct individual ecosystems due to the longitudinal fragmentation (Fellman et al. 2011; Vazquez et al. 2011; Siebers et al. 2015). However, the specific DOM sources and in-stream processes that provide this heterogeneity are still unknown. Moreover, such spatial heterogeneity in DOM composition may in turn imply variable DOM biodegradability along the river (e.g., Vazquez et al. 2011). Hence, DOM of different nature

(e.g., source and radiocarbon age) may be predominantly respired in each different aquatic environment.

Here we aimed at identifying the different sources of DOM and the DOM pools that were respired along a fragmented river under drought conditions. To do so, we characterized the DOM present in the different aquatic environments of a Mediterranean river during summer drought (isolated pools, running waters, and impounded waters in weirs) using a multi-faceted approach that combines absorbance-fluorescence spectroscopy, size-exclusion chromatography (SEC), biodegradation assays, and stable and radiocarbon isotope signatures of both organic and inorganic dissolved C (DOC and DIC, respectively). We expected (i) to identify heterogeneous DOM sources along the river, (ii) a partial disconnection from terrestrial DOM sources, and (iii) respiration of different DOM pools at each aquatic environment.

Methods

Study site

The Fluvià is a Mediterranean-type river located in the NE of the Iberian Peninsula (Fig. 1). Its main stem is 97 km long, with a mean flow of $3.6 \text{ m}^3 \text{ s}^{-1}$ in the basin outlet (data from 2004 to 2014; Catalan Water Agency). Its river network drains a 990 km^2 catchment covered by mixed forests (79 %) and agricultural (18 %) and urban (3 %) areas. The catchment geology is calcareous, with some areas (<15 %) of siliceous materials (Cartographic and Geological Institute of Catalonia, 2006). Climate is typically Mediterranean, with air temperatures ranging from 6 to $26 \text{ }^\circ\text{C}$ and a mean annual precipitation of 660 mm (data from 2004 to 2014; Catalan Water Agency) mainly occurring in autumn and spring with occasional summer storms. The hydrologic regime follows the precipitation pattern. During summer drought, the combination of scarce precipitation and high evapotranspiration promotes a drying pattern of the river network that begins in headwaters and advances downstream.

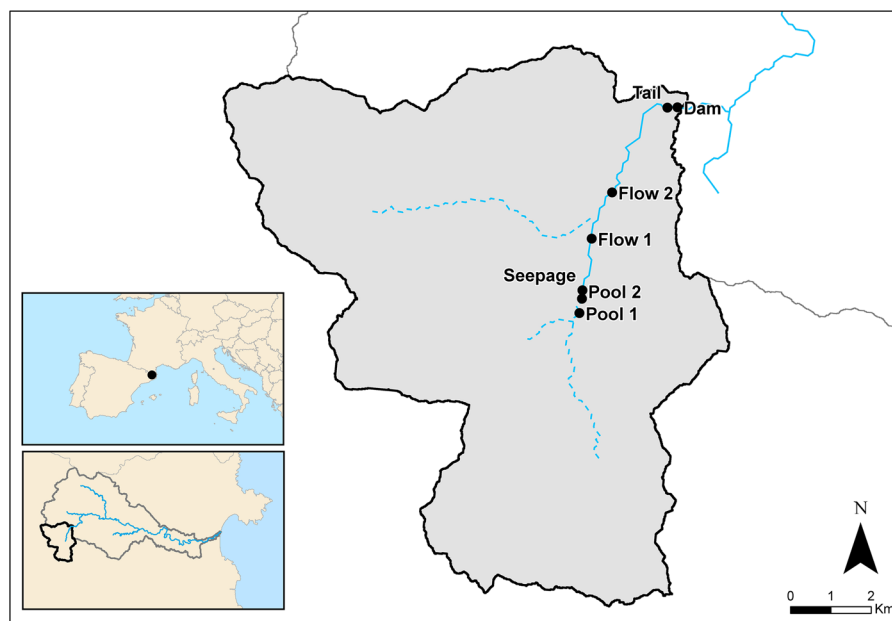
We focused this study on a 7-km upland reach of the Fluvià river main stem affected by drought during summer (Fig. 1). The study reach is surrounded by a dense deciduous riparian forest and croplands, with no influence of industrial or wastewater treatment activities. During the study period, the reach included upstream

isolated pools, 5.5 km of running waters, and the first weir on the main stem. We collected surface water from seven sites along the study reach representing these different aquatic environments. The selected sampling sites were two upstream isolated pools (“Pool1” and “Pool2”), the seepage point where groundwater appeared and surface water started to flow (“Seepage”), two downstream running water sites (“Flow1” and “Flow2”), and two sampling points in the weir: one just after the river water mixes with the lentic water body and the other near the dam (“Tail” and “Dam”, respectively; Fig. 1). Isolated pools were 500 m away from each other and were located in shaded areas under riparian canopy. Both pools contained several patches of accumulated tree leaves. However, whereas tree leaves accounted for 75 % of the Pool1 area, in Pool2 tree leaves only covered 10 %. Discharge progressively increased from Seepage to downstream running water sites, with no visible sudden changes along the study reach (Casas-Ruiz et al., personal observation). Discharge in Flow2 was $0.122 \text{ m}^3 \text{ s}^{-1}$ (Sontek, YSI, USA), with a mean water velocity of 0.07 m s^{-1} , and a width and mean water depth of 5.1 and 0.33 m, respectively. The substratum in both Flow1 and Flow2 was covered by epilithic and epipsammic biofilms. The area, volume and water residence time of the weir were 1.24 hm^2 , 0.0174 hm^3 and 1.65 days, respectively. The water depth in the weir was 0.6 m in Tail and 3.9 m in Dam.

Field sampling

Sampling was carried out in late summer (September the 1st, 2013) during a seasonal drought episode. Water samples for DOC and DIC concentrations (three samples per site) were collected with 60 mL syringes, immediately filtered in the field through pre-combusted and pre-rinsed $0.7 \text{ }\mu\text{m}$ glass fiber filters (GF/F; Whatman, UK), and placed without headspace into polyethylene plastic bottles after rinsing several times with filtered stream water. Samples for inorganic and organic C isotopes were collected without previous filtration in pre-cleaned (0.1 N HCl and Milli-Q) and combusted (4 h, $500 \text{ }^\circ\text{C}$) 2 L glass bottles, capped with solid ground glass joints. Inorganic C samples were stabilized in the field with mercury chloride solution. Samples for spectroscopic measurements and SEC were filtered in the field through pre-rinsed $0.2 \text{ }\mu\text{m}$ nylon filters (Whatman, UK) and placed into 11 mL polypropylene plastic containers (three

Fig. 1 Location of the sampling sites along the study reach. *Dashed lines* symbolize reaches that were dry during the sampling period. The *upper inset* shows the location of the Fluvià catchment in SW Europe. The *lower inset* shows the drainage area associated to the study reach within the Fluvià catchment (NE of the Iberian Peninsula)



samples per site). Water samples were kept in cool and dark conditions during transport to laboratory. Samples for DOC and DIC concentrations and spectroscopic measurements remained refrigerated ($<4\text{ }^{\circ}\text{C}$) in dark conditions, whereas those for SEC analyses were kept frozen until analysis. In addition, two samples of fresh leaves were collected in different locations along the study reach to estimate the ^{14}C signature of a recently produced terrestrial DOM source. We also used portable probes to measure in situ water temperature, conductivity, pH (WTW, Germany), and dissolved oxygen (DO; YSI ProODO Handheld, Ohio, USA) in each sampling site.

DOM characterization

We used DOC concentration as a quantitative indicator of DOM. All samples were analyzed for DOC concentration within one day following sample collection by high-temperature catalytic oxidation on a Shimadzu TOC-V CSH analyzer (Shimadzu Corporation, Japan).

Absorbance-fluorescence spectroscopy

UV–Vis absorbance spectra (190–800 nm) were measured on an Agilent 8453 diode array spectrophotometer (Agilent Technologies, Germany) using a 1-cm quartz cuvette. Milli-Q water was used as a

blank. The average sample absorbance between 700 and 800 nm was subtracted from the spectrum in order to correct for offsets due to instrument baseline drift (Green and Blough 1994). We calculated the specific UV absorbance at 254 nm (SUVA_{254} , $\text{L mg}^{-1} \text{m}^{-1}$), an indicator of aromatic C content (Weishaar et al. 2003), by dividing sample absorbance at 254 nm by DOC concentration and cell length.

Excitation-Emission matrices (EEMs) were obtained using a fluorescence spectrophotometer (F-7000, Hitachi, Japan) with a 1-cm quartz cuvette. EEMs were acquired by measuring fluorescence intensity across the excitation range set from 200 to 449 nm (3 nm increments) and the emission range set from 250 to 598 nm (3 nm increments). Excitation and emission slit widths were set to 5 nm. Water samples were allowed to warm to room temperature prior to measurements. All EEMs were read in ratio mode, whereby sample and lamp reference signal were corrected for instrument-specific biases after calibrating the instrument with Rhodamine B solution and the light diffuser and filter set provided by the manufacturer. EEMs were blank subtracted using the EEM of Milli-Q water collected every ten samples. Spectra were corrected for inner filter effects using UV–Visible absorbance spectra (Lakowicz 2006) without requiring previous dilution according to Kothawala et al. (2013). The integral of the Raman scatter peak of water blanks was used for intensity calibration following the procedure described in

Lawaetz and Stedmon (2009). EEMs were corrected and analyzed using MATLAB 2012a (Mathworks, MA, USA) software. We decided to interpret fluorescence data descriptively rather than by using any dimension reduction statistical approach (e.g., Zhang et al. 2014) because of the small size of our data set.

The intensity of the main fluorescence peaks related with DOM characterization (A, M, C, B, T; Coble 1996; Parlanti et al. 2000) was obtained from the EEMs. For each peak we kept the maximum fluorescence within the EEM regions defined in Fellman et al. (2010). Briefly, peaks A and C exhibit emission at long wavelengths and are related to aromatic humic-like fluorophores that derive from terrestrial sources. Peak M is also related to humic-like substances, although it exhibits emission at shorter wavelengths and is considered to be less aromatic and likely of lower molecular weight. Conversely, peaks B and T are related to tyrosine-like and tryptophan-like substances respectively, and have been associated to protein-like materials of different origin that are usually related to DOM lability (e.g., Balcarczyk et al. 2009; Guillemette and del Giorgio 2011). Fluorescence peak intensities are reported as percent contribution of each peak to the sum of fluorescence intensity by all peaks.

We also calculated the following spectral indices: the humification index (HIX), and the biological index (BIX). HIX was calculated as the ratio between the peak area under the emission spectra 435–480 nm and 300–345 nm, at an excitation wavelength of 254 nm (Zsolnay et al. 1999). HIX values increase with the extent of humification. BIX was calculated by dividing the fluorescence intensity emitted at 380 nm by that at 430 nm for an excitation of 310 nm (Huguet et al. 2009). Higher BIX values correspond to a higher autochthonous origin and to the presence of freshly released DOM (Huguet et al. 2009). We discarded the use of the fluorescence index (FI) because it showed a rather erratic behaviour in our samples, as previously reported in other studies (Korak et al. 2014).

Size-exclusion chromatography

The DOM size fractions were characterized by liquid chromatography. Briefly, the chromatographable DOC portion of the filtered samples passed through a size-exclusion column packed with resin (Toyopearl HW 50S, volume of 250 × 20 mm). Phosphate buffer (0,029 mol/L, pH 6,5) was used as eluent in a flow rate

of 1.1 ml min⁻¹. DOC was detected by infrared absorbance of CO₂ after UV oxidation at 185 nm in a cylindrical UV thin-film reactor (Graentzel-reactor). Fractions were identified by using fulvic and humic acid standards from the International Humic Substances Society (IHSS). In brief, the chromatograms were deconvoluted and apparent size fractions assigned based on the retention time and column affinity obtained for the IHSS standards. Fraction assignment was done by using the software FIFFIKUS (DOC-Labor Huber, Karlsruhe). We separated DOM into three different fractions: (i) high molecular weight substances (HMWS), including polysaccharides and to a lesser extent proteins or amino sugars, (ii) humic or humic-like substances (HS), including building blocks (lower molecular weight breakdown products of HS), and (iii) low molecular weight substances (LMWS), which includes low molecular weight acids and neutrals such as sugars and aminoacids. According to Her et al. (2002) HMWS corresponded to a molecular weight of 7 kDa or higher, HS to a range of 7–0.4 kDa, and LMWS to less than 0.4 kDa. We report each fraction as the percent contribution to total DOC.

Biodegradation assays

Biodegradable DOC (BDOC) was measured in dark incubations (Amon and Benner 1996; Guillemette and del Giorgio 2011). Briefly, we incubated 60 mL of filtered water (pre-rinsed 0.2 μm nylon membranes, Whatman, UK) with an inoculum added in a 1:10 proportion consisting in water from the same site filtered by Whatman GF/F. Samples were replicated three times and incubated in the dark in an incubation chamber at 20 °C for 65 days. BDOC was calculated as the difference in DOC prior and after the incubation.

Isotopic signatures

The δ²H and δ¹⁸O ratios of water samples were measured in the Colorado Plateau Stable Isotope Laboratory, Flagstaff, USA. For analysis of ¹³C in DOC (¹³C_{DOC}) and DIC (¹³C_{DIC}), separate water samples of 10 mL volume were stabilized with 10 μL HgCl₂ and sent to the Colorado Plateau Laboratory for conventional isotopic ratio mass spectrometry (MS). Samples for ¹⁴C_{DOC} and ¹⁴C_{DIC} were processed and

measured as described in Tittel et al. (2013). Briefly, DOC was filtered in the lab within 24 h after collection (pre-combusted Whatman GF/F) and then enriched at 60 °C by evaporation with UHP nitrogen. Inorganic C was outstripped after acidification and precipitated in barium hydroxide solution. $^{14}\text{C}_{\text{DOC}}$ and $^{14}\text{C}_{\text{DIC}}$ processed samples were measured by accelerator mass spectrometry (AMS) at the Leibniz-Laboratory for Radiometric Dating and Isotope Research in Kiel, Germany. Unfortunately, only three $\Delta^{14}\text{C}_{\text{DOC}}$ signatures (Pool1, Pool2, and Flow1) could be successfully determined. Flow2, Tail and Dam samples were lost at graphitization in the lab, while Seepage did not contain enough C. Data for stable isotopes is reported in standard δ notation (‰) relative to Vienna Standard Mean Ocean Water for $\delta^2\text{H}$ and $\delta^{18}\text{O}$, and standard Vienna Pee Dee Belemnite for ^{13}C . ^{14}C data is reported in Δ notation with respect to oxalic acid II standard and corrected for isotope fractionation (Stuiver and Polach 1977). Inorganic C isotopic signatures were measured on unfiltered samples; however, we refer to them as $^{13}\text{C}_{\text{DIC}}$ and $^{14}\text{C}_{\text{DIC}}$ throughout the manuscript because data from previous samplings indicate that particulate inorganic C represents less than 1 % of total inorganic C in the study reach (Casas-Ruiz, unpublished data).

Influence of CO_2 outgassing on $\delta^{13}\text{C}_{\text{DIC}}$

We evaluated the potential drift in $\delta^{13}\text{C}_{\text{DIC}}$ values due to gas exchange along the running water reaches. To do this, we estimated the DIC evaded as CO_2 between consecutive stations. Then, we solved a simple isotope mixing model to estimate the downstream $\delta^{13}\text{C}_{\text{DIC}}$ using the observed upstream $\delta^{13}\text{C}_{\text{DIC}}$ and the mass of DIC evaded as CO_2 .

Based on the Fick's First Law of diffusion, the gas exchange at the water–air interface is driven by the reaeration coefficient and the gas concentration gradient. Hence, we calculated the DIC change within the reaches as

$$\frac{\partial \text{DIC}}{\partial t} = k z^{-1} \Delta \text{CO}_2 \quad (1)$$

where $\frac{\partial \text{DIC}}{\partial t}$ is the variation in DIC concentration with time ($\text{mol L}^{-1} \text{s}^{-1}$), k is the gas transfer velocity (m s^{-1}), z is the water depth (m) and ΔCO_2 is the gradient between the concentration of CO_2 in the water and in the atmosphere (mol L^{-1}). The physical

parameter k was obtained by applying the night-time regression method (Hornberger and Kelly 1975) on dissolved oxygen data measured every 10 min in Flow2 (mean of 4 nights). Water depth z was calculated as the mean depth from Seepage to Tail using an HEC-RAS model fed with the discharge in Flow2 and reach cross sections measured every ca. 100 m. Initial ΔCO_2 was calculated using the measured DIC and pH of each reach upstream station, assuming an atmospheric CO_2 partial pressure of 390 ppm_v. Then, we iteratively computed ΔCO_2 and DIC concentrations implementing Eq. 1 in the CO2SYS software (Lewis and Wallace 1998). The final DIC concentration in the downstream station was the DIC concentration after a time lapse equal to the travel time of the water in the reach. Once the DIC evasion between stations was obtained, we applied a simple isotope mixing model to calculate the resulting downstream $\delta^{13}\text{C}_{\text{DIC}}$. Since bicarbonate was the predominant DIC fraction (>90 %) and there were no major changes in pH along the running water reaches (Table 1), we assumed an enrichment factor between DIC and $\text{CO}_{2(\text{g})}$ of -9 ‰ at 15 °C (Zhang et al. 1995). The comparison between the resulting $\delta^{13}\text{C}_{\text{DIC}}$ due to CO_2 outgassing alone and the measured $\delta^{13}\text{C}_{\text{DIC}}$ value in the downstream station informs about the relevance of outgassing versus other potential processes on the increasing $\delta^{13}\text{C}_{\text{DIC}}$ values.

Data treatment and analysis

We report data in this study as the mean and standard deviation of each variable based upon three real replicates. In the case of isotope signatures and SEC fractions, values are reported as the mean and deviation (0.5 range) of two real replicates for SEC and $\delta^{13}\text{C}$, and of two analytical replicates for $\Delta^{14}\text{C}$. We applied Spearman correlation tests to analyze the relationship between variables. All statistical analyses were run in R 3.1.3 (R Core Team 2015).

Results

Water physicochemistry

River water $\delta^2\text{H}$ and $\delta^{18}\text{O}$ values (Table 1) ranged from -41.8 to -27.5 ‰ and from -6.8 to -5.1 ‰, respectively, and divided the study sites in two

Table 1 Water physicochemical parameters in the sampling sites

	$\delta^2\text{H}$ (‰) ^a	$\delta^{18}\text{O}$ (‰) ^a	T (°C)	pH	DO (%)	Cond ($\mu\text{S cm}^{-1}$)	DIC ^b (mg C L^{-1})
Pool	−29.0 (0.1)	−5.4 (0.0)	16.4	7.3	17.4	344	35.6 ± 0.4
Pool2	−27.5 (0.0)	−5.1 (0.0)	16.5	7.2	2.7	336	32.3 ± 0.1
Seepage	−30.1 (0.1)	−5.5 (0.0)	16.6	7.2	49.6	564	59.0 ± 0.7
Flow1	−40.4 (0.0)	−6.7 (0.1)	15.1	7.7	81	724	75.5 ± 0.3
Flow2	−41.8 (0.0)	−6.7 (0.0)	16.0	7.7	112.8	610	65.7 ± 0.2
Tail	−41.0 (0.0)	−6.7 (0.0)	16.9	8.2	96.9	522	57.3 ± 0.8
Dam	−38.9 (0.1)	−6.8 (0.2)	16.0	8.2	77.6	506	62.7 ± 0.2

^a Mean and 0.5 range (in brackets) of duplicate samples

^b Mean and standard deviation of three real replicates

T water temperature; Cond conductivity; DO dissolved oxygen

different groups: (i) the isolated pools and Seepage, and (ii) the running water sites and the weir (Fig. 2). All water samples showed very low deviation from the Local Meteoric Water Line of the Montseny area (40 km from the study area; Neal et al. 1992). No significant evidences of evaporation during soil infiltration and transport to the river channel or within the river were observed.

Water temperature was relatively stable along the study reach, with the lowest value in Flow1 (15.1 °C) and the highest in Tail (16.9 °C; Table 1). The pH varied from 7.2 to 8.2, showing lowest values in

isolated pools and an increasing trend from Seepage to Dam. DO saturation widely varied across sites (from 3 % in Pool2 to 112 % in Flow2), and showed an increasing trend from Seepage to Flow2. Conductivity ranged from 336 to 724 $\mu\text{S cm}^{-1}$, with the lowest values in isolated pools and the highest value in Flow1. DIC concentrations ranged from 32.3 to 75.5 mg C L^{-1} , and followed a similar pattern to that of conductivity.

DOM quantity and composition

DOM quantity was highly variable along the study reach. DOC concentration ranged from 1.0 to 4.2 mg C L^{-1} , with the highest values found in the two isolated pools and the lowest in Flow2 (Table 2). Similarly, the qualitative characterization of DOM by absorbance-fluorescence spectroscopy indicated large variation in DOM composition across sites (Table 2). SUVA_{254} varied from 2.0 in Flow2 to 3.0 $\text{L mg C}^{-1} \text{m}^{-1}$ in Pool2 and Seepage, corresponding to an aromatic content of ~16 to 23 % according to Weishaar et al. (2003). HIX values widely ranged from 4.0 to 8.3, presenting the lowest values in running waters (Flow1 and Flow2) and the highest value in the tail of the weir. BIX ranged from 0.65 in Tail to 0.79 in Flow1, showing an opposite pattern to that of HIX (Fig. 3). All water samples were dominated by humic-like fluorescence, with peak A representing more than 40 % of the fluorescence derived from the combination of the five peaks in all sites. Contribution of peaks A, M, and C was relatively homogeneous across sites, showing a coefficient of variation of 5, 2, and 6 % respectively. Conversely, protein-like peaks T and B

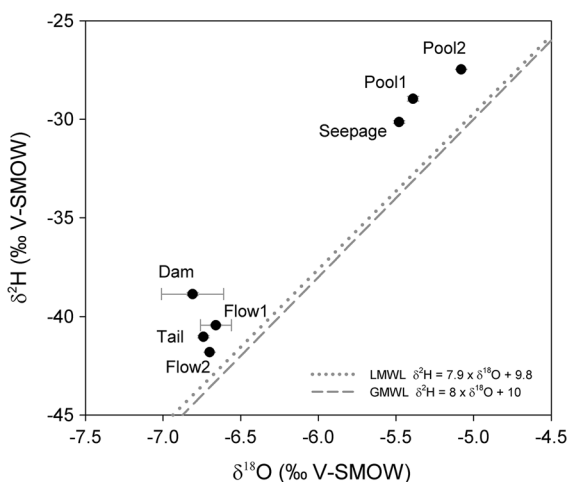


Fig. 2 Relationship between $\delta^{18}\text{O}$ and $\delta^2\text{H}$ for the water samples. The global meteoric water line (GMWL) and the local meteoric water line of the Montseny area (LMWL; Neal et al. 1992) are shown. Error bars symbolize the 0.5 range of duplicate samples. Note that in some cases error bars are behind the symbol. V-SMOW; Vienna Standard Mean Ocean Water

Table 2 Dissolved organic carbon concentration and absorbance-fluorescence descriptors of DOM composition across sites (Mean \pm SD)

	DOC (mg C L ⁻¹)	SUVA ₂₅₄ (L mg C ⁻¹ m ⁻¹)	HIX	BIX	Peak A (%)	Peak M (%)	Peak C (%)	Peak B (%)	Peak T (%)
Pool1	3.8 \pm 0.1	3.0 \pm 0.1	6.6 \pm 0.0	0.68 \pm 0.00	46.0 \pm 0.1	21.8 \pm 0.2	18.7 \pm 0.1	3.7 \pm 0.2	9.7 \pm 0.0
Pool2	4.2 \pm 0.1	2.7 \pm 0.0	6.5 \pm 0.2	0.70 \pm 0.00	43.7 \pm 0.2	21.9 \pm 0.2	21.6 \pm 0.2	3.7 \pm 0.3	9.2 \pm 0.1
Seepage	1.3 \pm 0.0	3.0 \pm 0.1	7.1 \pm 0.4	0.74 \pm 0.01	48.7 \pm 0.5	22.2 \pm 0.1	19.0 \pm 0.7	2.3 \pm 0.0	7.9 \pm 0.3
Flow1	1.3 \pm 0.0	2.1 \pm 0.2	4.2 \pm 0.1	0.79 \pm 0.01	43.7 \pm 0.3	21.8 \pm 0.6	19.0 \pm 0.0	4.5 \pm 0.5	11.1 \pm 0.8
Flow2	1.0 \pm 0.0	2.0 \pm 0.2	4.0 \pm 0.4	0.77 \pm 0.00	44.4 \pm 1.0	22.3 \pm 1.3	18.2 \pm 0.3	4.2 \pm 1.2	11.0 \pm 0.5
Tail	2.2 \pm 0.0	2.7 \pm 0.1	8.3 \pm 0.4	0.65 \pm 0.01	49.3 \pm 1.0	23.1 \pm 0.3	18.9 \pm 0.2	2.4 \pm 0.3	6.3 \pm 0.4
Dam	1.7 \pm 0.0	2.2 \pm 0.1	6.8 \pm 0.6	0.67 \pm 0.01	47.8 \pm 1.8	22.9 \pm 0.8	18.0 \pm 0.4	3.0 \pm 0.9	8.3 \pm 1.2

Fluorescence peaks are reported as percent contribution of each peak to the sum of fluorescence intensity by all peaks

SUVA₂₅₄ specific UV absorbance at 254 nm; HIX humification index; BIX biological index

showed relatively high heterogeneity (coefficient of variation of 19 and 25 %, respectively), with highest values in Flow1 and Flow2 and lowest in Tail.

SEC analyses indicate that LMWS was the dominant fraction in the running water sites and in Dam (Table 3). Conversely, isolated pools, Seepage, and Tail were dominated by HS. Only isolated pools showed relatively high contributions of HMWS (7.3 and 7.6 % in Pool1 and Pool2, respectively). The percentage of HS correlated positively with SUVA₂₅₄ ($r_s = 0.79$, $p < 0.05$) and HIX ($r_s = 0.71$, $p = 0.09$).

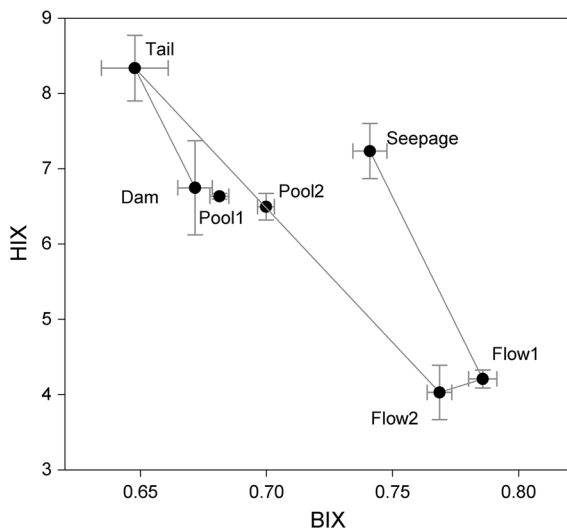


Fig. 3 Relationship between biological index (BIX) and humification index (HIX) across sampling sites. The continuous line follows the longitudinal flow direction from the Seepage site to the weir. Note that the position of Pool2 over the line is accidental

A more detailed comparison between SEC and absorbance-fluorescence results is shown in Table 4.

The percentage of BDOC ranged from 11 to 42 % (Table 3). DOM in running waters showed the highest biodegradability, while Tail had the least bioavailable DOM along the study reach. Overall, the percentage of BDOC decreased with increasing HIX and the percentage of HS ($r_s = -0.78$, $p < 0.05$ and $r_s = -0.82$, $p < 0.05$, respectively; Fig. 4a) as well as SUVA₂₅₄ ($r_s = -0.85$, $p < 0.05$). Conversely, there was a positive correlation between the percentage of BDOC and the percentage of LMWS ($r_s = 0.89$, $p < 0.05$; Fig. 4b) and a marginally significant relationship between the percentage of BDOC and protein-like peak T ($r_s = 0.75$, $p = 0.07$; Fig. 4c).

Isotopic signatures

C isotopic signatures of DOC and DIC are given in Table 5. $\Delta^{14}\text{C}_{\text{DOC}}$ ranged from -108 to -158 ‰, corresponding to a conventional radiocarbon age (CRA) of 855 to 1318 year B.P. $\Delta^{14}\text{C}_{\text{DOC}}$ of riparian leaves (21 ‰) corresponded to a modern origin (i.e., produced after 1950). $\delta^{13}\text{C}_{\text{DOC}}$ values showed little variability along the study reach, with values ranging from -28.2 ‰ in Seepage to -26.0 ‰ in Pool1. $\Delta^{14}\text{C}_{\text{DIC}}$ ranged from -1 ‰ in Pool1 to -52 ‰ in Flow2 and Tail, corresponding to CRA of Modern to 370 year B.P. $\delta^{13}\text{C}_{\text{DIC}}$ values varied from -13.3 to -9.6 ‰ (Fig. 5), showing a ^{13}C enrichment as water flowed downstream, and a positive relationship with DO saturation ($r_s = 0.77$, $p < 0.05$). Assuming CO_2

Table 3 Size fractions of dissolved organic matter and proportion of biodegradable dissolved organic carbon (BDOC) in the sampling sites

	HMWS ^a (%)	HS ^a (%)	LMWS ^a (%)	BDOC ^b (%)
Pool1	6.6 (0.8)	66.8 (4.4)	26.5 (5.5)	26 ± 1
Pool2	7.3 (0.1)	57.6 (12.8)	35.5 (12.5)	32 ± 3
Seepage	0.3 (0.4)	56.9 (8.0)	42.9 (7.8)	29 ± 2
Flow1	2.3 (0.1)	35.1 (1.0)	63.0 (1.0)	42 ± 4
Flow2	1.1 (0.2)	30.8 (5.3)	68.0 (5.0)	41 ± 0
Tail	2.0 (0.1)	67.2 (0.4)	31.0 (0.0)	11 ± 8
Dam	2.8 (0.1)	49.3 (0.9)	48.0 (1.0)	35 ± 5

Reported values are percent contribution to total dissolved organic carbon

^a Mean and 0.5 range (in brackets) of duplicate samples measured by size-exclusion chromatography

^b Mean ± standard deviation of triplicate samples

Table 4 Spearman correlations between absorbance-fluorescence descriptors and size-exclusion chromatography fractions

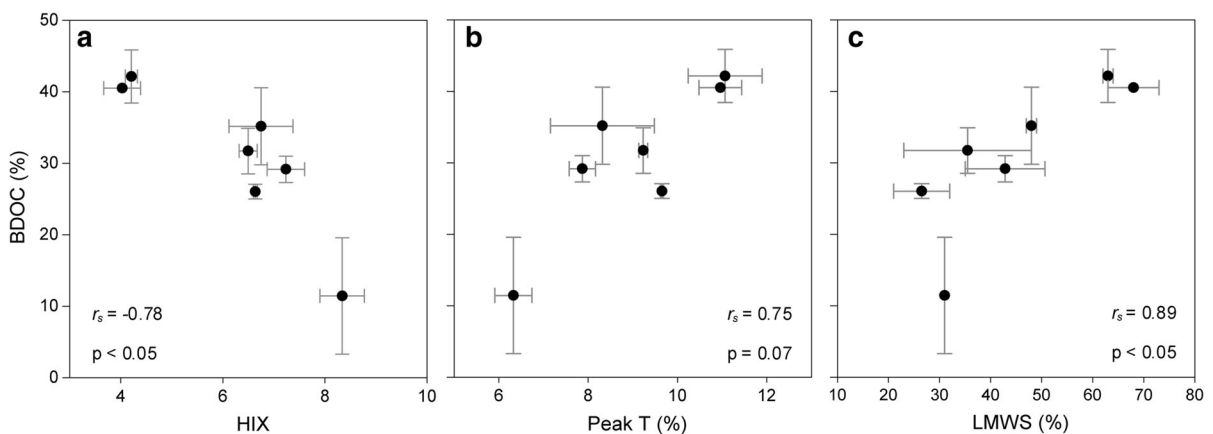
	HMWS (%)	HS (%)	LMWS (%)
SUVA ₂₅₄	0.05	0.79*	-0.85*
BIX	-0.29	-0.75*	0.68
HIX	-0.18	0.71	-0.61
% Peak A	-0.49	0.49	-0.38
% Peak C	0.13	0.25	-0.22
% Peak M	-0.4	0.11	0.09
% Peak T	0.21	-0.64	0.5
% Peak B	0.31	-0.56	0.47

Asterisk indicate statistical significance ($\alpha = 0.05$)

outgassing as the only process governing $\delta^{13}\text{C}_{\text{DIC}}$ along the running water sites, we estimated hypothetical $\delta^{13}\text{C}_{\text{DIC}}$ values of -11.5 and -11.1 ‰ in Flow1 and Flow2, respectively (see “Methods” for calculation details). The comparison of these values with the measured ones (Table 5) suggests that CO_2 outgassing might explain about 60 % of the overall $\delta^{13}\text{C}_{\text{DIC}}$ increase along the running water sites.

Discussion

The lack of hydrological connectivity determined the different sources of DOM as well as its degradation

**Fig. 4** Relationship between the percentage of biodegradable dissolved organic carbon (BDOC) and **a** the humification index (HIX), **b** the percentage of low molecular weight substances

(LMWS), and **c** the percentage of protein-like Peak T. Results from Spearman correlation tests are shown

Table 5 Stable and radiocarbon isotopic signatures of dissolved organic carbon (DOC) and dissolved inorganic carbon (DIC) across the study sites

	$\delta^{13}\text{C}_{\text{DOC}}$ (‰) ^a	$\delta^{13}\text{C}_{\text{DIC}}$ (‰) ^a	$\Delta^{14}\text{C}_{\text{DOC}}$ (‰) ^a	$\Delta^{14}\text{C}_{\text{DOC}}$ age (year B.P.) [*]	$\Delta^{14}\text{C}_{\text{DIC}}$ (‰) ^a	$\Delta^{14}\text{C}_{\text{DIC}}$ age (year B.P.) [*]
Pool 1	−26.0 (0.0)	−12.8 (0.1)	−108(4)	855	−1 (3)	Modern
Pool 2	−26.2 (0.0)	−13.3 (0.0)	−125 (3)	1010	−33 (3)	204
Seepage	−28.2 (0.0)	−12.3 (0.0)	NA ^{††}	–	−34 (3)	217
Flow1	−26.8 (NA)	−11.4 (0.0)	−158 (5)	1318	−38 (3)	249
Flow2	−26.7 (NA)	−10.5 (0.3)	NA [†]	–	−52 (3)	371
Tail	−27.0 (0.1)	−10.5 (0.0)	NA [†]	–	−52 (3)	372
Dam	−26.9 (0.1)	−9.6 (0.2)	NA [†]	–	−34 (3)	213

NA not available

[†] Lost at graphitization (See “Methods” section)

^{††} Sample did not contain enough C to measure $\Delta^{14}\text{C}$ signature

^{*} The C ages are given as conventional radiocarbon age (CRA; Stuiver and Polach 1977). B.P. refers to years before 1950

^a The values of $\Delta^{14}\text{C}$ (mean of two analytical replicates (0.5 range)) and of $\delta^{13}\text{C}$ (mean of duplicates (0.5 range)) express the isotopic signatures as per mil deviation relative to analytical standards (See “Methods” section)

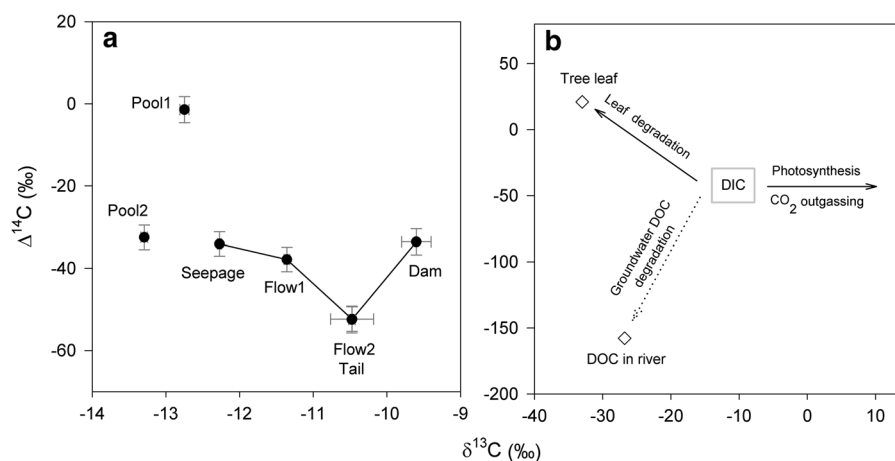


Fig. 5 Stable and radiocarbon isotopic signatures of dissolved inorganic carbon (DIC) across sites (a) and projected isotopic changes for processes affecting DIC in our study case (b). The grey square in b represents the range of $\delta^{13}\text{C}_{\text{DIC}}$ and $\Delta^{14}\text{C}_{\text{DIC}}$ in the flow-connected sites (i.e., from Seepage to Dam). Potential sources of DIC include degradation of tree leaves ($\delta^{13}\text{C}$ ca. −33 ‰, $\Delta^{14}\text{C}$ 21 ‰) and degradation of old river DOC

(assumed similar to DOC in Flow1, i.e., $\delta^{13}\text{C}$ −28 ‰ and $\Delta^{14}\text{C}$ −158 ‰). Carbonate dissolution was not considered a potential DIC source since high and increasing pH values were found along the study reach. Error bars in a represent the 0.5 range of duplicate samples for $\delta^{13}\text{C}$ and 0.5 range of duplicate analyses for $\Delta^{14}\text{C}$

along the river. The old DOC measured in the study reach (855 to 1318 year B.P.) suggests that groundwater from relatively deep soil horizons was feeding the channel (Trumbore and Schiff 1992; Neff et al. 2006; Butman et al. 2007), likely caused by hydrological disconnection of the river from the riparian zone and the shallow subsurface flow (Dahm et al. 2003; Lake 2003). This lateral flow disconnection

influenced the DOM sources along the study reach, and the longitudinal fragmentation promoted by flow cessation provided distinct individual environments in terms of physicochemistry and DOM properties. As a result, we found highly contrasting values of DOM descriptors and physicochemical parameters along just seven kilometres of river reach. For instance, the percentage of BDOC spanned from 11 to 42 %, a

range that is comparable to or higher than the range in BDOC found across different rivers (del Giorgio and Davis 2003; Balcarczyk et al. 2009; Fellman et al. 2009, 2014). Such heterogeneity is consistent with previous studies in temporary rivers from Mediterranean (Vazquez et al. 2011; von Schiller et al. 2015) and other semiarid regions (Fellman et al. 2011; Siebers et al. 2015), where an enhanced variability of DOM composition as well as water physicochemistry occurs during hydrological fragmentation.

The physicochemical parameters measured along the river suggest that groundwater with different characteristics than Seepage contributed to the river flow (e.g., note the different $\delta^2\text{H}$, $\delta^{18}\text{O}$ and Cond between Seepage and Flow1, Table 1). In this sense, part of the observed heterogeneity in DOM and physicochemical parameters could derive from the mixing with non-sampled groundwater. Nevertheless, the small variation in $\delta^2\text{H}$ and $\delta^{18}\text{O}$ from Flow1 to Dam (Table 1, Fig. 2) indicates that subsurface inputs promoting the perceived flow increase along the river derived all from the same source. Hence, in-stream processes might have played a relevant role on the observed relative changes in DOM and water chemistry between these sites.

Spatial discontinuities in DOM sources along the river

One of the more conspicuous heterogeneities in our data set emerges from the rapid increase in protein-like, low molecular weight DOM along the running water sites, which suggests an increasing influence of algal/bacterial DOM sources (Bertilsson and Jones 2003). Accordingly, the position of Flow1 and Flow2 in the BIX-HIX plane (Fig. 3) shows an enrichment of fresh and low-humified DOM from the Seepage site to downstream running waters, also indicated by a decrease in SUVA_{254} . These results are in line with recent findings in Mediterranean temporary rivers, where a decrease in the proportion of terrestrial versus autochthonous DOM has been described during the contraction and fragmentation phases of drought (Vazquez et al. 2011; Ylla et al. 2011; von Schiller et al. 2015). However, we cannot identify the ultimate origin of this algal/bacterial DOM, because both autochthonous sources as well as groundwater DOM inputs between Seepage and Flow1 with a strong microbial signal (e.g., Birdwell

and Engel 2010) could explain the observed shift in DOM composition.

In any case other evidences suggest that autochthonous DOM contributions, algal primary production in particular, were significant along these sites. The increase in $\delta^{13}\text{C}_{\text{DIC}}$ from Flow1 to Flow2 suggests that in-stream processes affecting the DIC isotopic signal took place within the running water sites (Fig. 5). Our rough estimation of the CO_2 evaded along the running water sites indicates that CO_2 outgassing could explain up to 60 % of the observed $\delta^{13}\text{C}_{\text{DIC}}$ increase, so this process alone cannot explain the overall $\delta^{13}\text{C}_{\text{DIC}}$ trend. Consequently, considering that carbonates dissolution is unlikely given the high and increasing pH (Table 1), photosynthesis must have been a relevant process in the running water sites, also supported by oxygen increasing above saturation in Flow2 (112 %).

The most contrasting sites in terms of DOM properties were, however, the upstream isolated pools, where we found the highest DOC concentrations. The DOM fluorescence properties and molecular weight fractions indicate that the pools were dominated by terrestrially derived, humic compounds with lower contributions of LMWS in comparison to the flow-connected sites. Such a terrestrial character is likely related to the leaching and degradation of the accumulated riparian tree leaves (see sites description), which is consistent with their relatively high proportion of HMWS (Meyer et al. 1998; Francis and Sheldon 2002). Also, the relatively young DOC radiocarbon ages compared to that in Flow1 (Table 5) are in agreement with contributions of DOC by degradation of tree leaves ($\delta^{13}\text{C}_{\text{POC}} -33 \text{‰}$, $\Delta^{14}\text{C}_{\text{POC}} 21 \text{‰}$). Indeed, tree leaves and detritus usually accumulate in isolated pools due to lack of advection (Acuña et al. 2005; Bond et al. 2008; von Schiller et al. 2011), causing high DOC concentrations and fuelling respiration (Sabater and Tockner 2010). In our case, the lower $\delta^{13}\text{C}_{\text{DIC}}$ values measured in the pools in comparison to the flow-connected sites accordingly suggest high respiration activity (Fig. 5), also indicated by the very low DO levels (2.7 and 17.4 % in Pool1 and 2, respectively). Therefore, our results suggest that leaf degradation may be the main DOM source in the pools. Nevertheless, the hydrological isolation of the pools makes them independent systems that are highly influenced by their particular local conditions. Therefore, our observations would probably differ under different situations such as less

canopy cover and so less leaf inputs and higher light availability, whereby algal DOM sources may increase (Dahm et al. 2003; Fellman et al. 2011).

The tail of the weir constitutes another clear discontinuity along the study reach. The BIX-HIX plane (Fig. 3) displays Tail in the opposite corner of the immediately upstream-located running waters, which is consistent with the highest $SUVA_{254}$ and percentage of HS along the study reach. This, in combination with low BDOC (11 %), indicates a highly degraded DOM in this site. The tail of weirs and impoundments where river water mixes with the lentic water body can be a high degradation environment (Šimek et al. 2010), strongly influenced by the activity of the accumulated sediment (Cardoso et al. 2013). In fact, fluxes from the sediment to the water column can be highly influential on the river chemistry during low flow periods (Mosley 2015). Hence, based on DOM composition data, we suggest both intense degradation of fresh DOM and release of highly degraded DOM from the sediment to be responsible for the humified character in this particular site. However, this interpretation is not clearly supported by physicochemical data (e.g., there is no marked $\delta^{13}C_{DIC}$ depletion in Tail; Fig. 5).

Spatial discontinuities in DOM degradation along the river

The relationships between BDOC and the optical and chemical properties of DOM indicate a microbial preference for protein-like, fresh, low molecular weight DOM (Fig. 4). These results pose autochthonous DOM as the most bioavailable DOM, and suggest that it may cycle rapidly within the river. However, because of the experimental *ex situ* approach we used, BDOC values provide information about the potential bioavailability of DOM rather than its actual *in situ* degradation. Therefore, in order to further recognize the DOM pools that were being degraded in each aquatic environment, we compared the variation in DIC isotopic signatures among sites (Fig. 5).

Mineralization-derived CO_2 reflects the isotopic signal of the organic matter source. Hence, since we identified leaf leachates, algal release, and groundwater inputs as the principal DOM sources along the study reach, we considered them as the end-members whose degradation could modify the riverine $\Delta^{14}C_{DIC}$. Following this approach and departing from a $\Delta^{14}C_{DIC}$ range of -34 to -52 ‰ in the flow-connected sites,

inputs of CO_2 resulting from the *in situ* degradation of tree leaves ($\Delta^{14}C_{POC} = 21$ ‰) along the river would increase water $\Delta^{14}C_{DIC}$ values (Fig. 5b). Differently, inputs of CO_2 due to the degradation of algal DOM should not greatly affect $\Delta^{14}C_{DIC}$ values, because $\Delta^{14}C$ of photosynthetically derived DOC reflects that of the DIC available for C fixation. Finally, assuming the old DOC measured in Flow1 ($\Delta^{14}C_{DOC} = -158$ ‰; Table 5) derives from groundwater inputs, degradation of groundwater DOM within the river should decrease $\Delta^{14}C_{DIC}$ values.

Two distinct patterns of $\Delta^{14}C_{DIC}$ variation were therefore observed along the study reach. On the one hand, leaf degradation appeared to be a relevant process in isolated pools, as indicated by the higher $\Delta^{14}C_{DIC}$ in comparison to the flow-connected sites (Fig. 5). This is in agreement with their identification as high respiration environments (see above), and at the same time supports that the HMWS and the high DOC concentrations measured in the pools derived from the degradation of leaves. Consistently, riparian litterfall leachates have been previously suggested as a labile DOM source to rivers, especially its highest molecular weight fractions (McArthur and Richardson 2002; Romani et al. 2006; Vazquez et al. 2015). Noteworthy, the increase in $\Delta^{14}C_{DIC}$ from Tail to Dam suggests that leaf leachate degradation also occurred in the weir (Fig. 5), overall emphasizing the role of tree leaves from overhanging canopies as a relevant DOM source as well as an energy substrate for aquatic heterotrophs in sites with high water residence time.

On the other hand, degradation of groundwater old DOM likely occurred within the river, as indicated by the $\Delta^{14}C_{DIC}$ depletion from Seepage to Tail (Fig. 5). This result is consistent with recent evidence for the respiration of aged DOM in glacier (Singer et al. 2012), boreal (McCallister and Del Giorgio 2012) and tropical ecosystems (Fellman et al. 2014), suggesting a biogeochemical link between past C fixation and contemporary river metabolism. Nevertheless, we cannot discern whether the $\Delta^{14}C_{DIC}$ decrease in our reach results from (i) degradation of significant amounts of moderately aged DOM, or (ii) from sporadic degradation of strongly ^{14}C -depleted DOM. Also, we cannot fully discard that inputs of groundwater old DIC contributed to the observed $\Delta^{14}C_{DIC}$ depletion along the river. In any case, the positive correlations found between the percentage of BDOC and protein-like, fresh, low molecular weight DOM

(Fig. 4) suggest a microbial preference for the algal/bacterial DOM measured in the running water sites. Thus, both groundwater millennial DOM and autochthonous DOM could be simultaneously degraded along the running water sites.

Conclusions

The lack of hydrological connectivity caused by drought implied a spatial discontinuity in the DOM sources along the study reach, determining at the same time the DOM pool that was being respired in each aquatic environment. The partial isolation of the river from its catchment promoted a relevant influence of autochthonous DOM sources. However, although terrestrial inputs from the riparian zone can be notably reduced, tree leaves from overhanging canopies stood out as an important bioavailable DOM source, especially in sites where water residence time was high (isolated pools and weirs). Groundwater millennial DOM (>1300 year B.P.) seemed to be respired within the river, suggesting a biogeochemical link between past C fixation and contemporary river metabolism. Although our results are inherently subject to regional and local factors that may widely differ between regions, rivers, and even reaches, they highlight a highly heterogeneous DOM pool during drought, with special emphasis on the role of local conditions (e.g., differences in light and riparian leaves availability) that may hinder any spatial upscaling.

Acknowledgments This research was funded by the Spanish Ministry of Economy and Competitiveness through the project CARBONET (CGL2011-30474-C02-01). J. P. Casas-Ruiz and Ll. Gómez-Gener were additionally supported by FPI predoctoral grants (BES-2012-059655 and BES-2012-059743), and D. von Schiller by a “Juan de la Cierva” postdoctoral grant (JCI-2010-06397). N. Catalán held a Wenner-Gren foundation stipend (Sweden). Authors also acknowledge the support from the Economy and Knowledge Department of the Catalan Government through Consolidated Research Group (2014 SGR 291)—Catalan Institute for Water Research. We thank Lorenzo Proia, Yvonne Rosenlöcher, Meritxell Abril, Susanne Halbedel, and Carmen Gutiérrez for lab and field assistance.

References

- Acuña V, Muñoz I, Giorgi A et al (2005) Drought and post-drought recovery cycles in an intermittent Mediterranean stream: structural and functional aspects. *J North Am Benthol Soc* 24:919–933
- Aitkenhead-Peterson JA, McDowell WH, Neff JC (2003) Sources, production, and regulation of allochthonous dissolved organic matter inputs to surface waters. In: Findlay S, Sinsabaugh R (eds) *Aquatic ecosystems: interactivity of dissolved organic matter*. Academic Press, Elsevier, pp 26–70
- Amon RMW, Benner R (1996) Bacterial utilization of different size classes of dissolved organic matter. *Limnol Oceanogr* 41:41–51
- Balcarczyk KL, Jones JB Jr, Jaffé R, Maie N (2009) Stream dissolved organic matter bioavailability and composition in watersheds underlain with discontinuous permafrost. *Biogeochemistry* 94:255–270. doi:10.1007/s10533-009-9324-x
- Battin TJ, Kaplan LA, Findlay S et al (2008) Biophysical controls on organic carbon fluxes in fluvial networks. *Nat Geosci* 1:95–100. doi:10.1038/ngeo101
- Benner R (2003) Molecular indicators of the bioavailability of dissolved organic matter. In: Findlay S, Sinsabaugh R (eds) *Aquatic ecosystems: interactivity of dissolved organic matter*. Academic Press, Elsevier, pp 121–137
- Bernal S, Schiller D, Sabater F, Martí E (2013) Hydrological extremes modulate nutrient dynamics in mediterranean climate streams across different spatial scales. *Hydrobiologia* 719:31–42. doi:10.1007/s10750-012-1246-2
- Bertilsson S, Jones JB (2003) Supply of dissolved organic matter to aquatic ecosystems: Autochthonous sources. In: Findlay S, Sinsabaugh R (eds) *Aquatic ecosystems: interactivity of dissolved organic matter*. Academic Press, Elsevier, pp 3–24
- Birdwell JE, Engel AS (2010) Characterization of dissolved organic matter in cave and spring waters using UV–Vis absorbance and fluorescence spectroscopy. *Org Geochem* 41:270–280. doi:10.1016/j.orggeochem.2009.11.002
- Bond NR, Lake PS, Arthington AH (2008) The impacts of drought on freshwater ecosystems: an Australian perspective. *Hydrobiologia* 600:3–16. doi:10.1007/s10750-008-9326-z
- Butman D, Raymond P, Oh N-H, Mull K (2007) Quantity, ^{14}C age and lability of desorbed soil organic carbon in fresh water and seawater. *Org Geochem* 38:1547–1557. doi:10.1016/j.orggeochem.2007.05.011
- Butman D, Raymond PA, Butler K, Aiken G (2012) Relationships between $\Delta^{14}\text{C}$ and the molecular quality of dissolved organic carbon in rivers draining to the coast from the conterminous United States. *Global Biogeochem Cycles*. doi:10.1029/2012GB004361
- Caraco N, Bauer JE, Cole JJ et al (2010) Millennial-aged organic carbon subsidies to a modern river food web. *Ecology* 91:2385–2393. doi:10.1890/09-0330.1
- Cardoso SJ, Vidal LO, Mendonça RF et al (2013) Spatial variation of sediment mineralization supports differential CO_2 emissions from a tropical hydroelectric reservoir. *Front Microbiol* 4:101. doi:10.3389/fmicb.2013.00101
- Coble PG (1996) Characterization of marine and terrestrial DOM in seawater using excitation-emission matrix spectroscopy. *Mar Chem* 51:325–346
- Cole JJ, Caraco NF (2001) Carbon in catchments: connecting terrestrial carbon losses with aquatic metabolism. *Mar Freshw Res* 52:101–110

- Cole JJ, Prairie YT, Caraco NF et al (2007) Plumbing the global carbon cycle: integrating inland waters into the terrestrial carbon budget. *Ecosystems* 10:172–185. doi:[10.1007/s10021-006-9013-8](https://doi.org/10.1007/s10021-006-9013-8)
- Dahm CN, Baker MA, Moore DI, Thibault JR (2003) Coupled biogeochemical and hydrological responses of streams and rivers to drought. *Freshw Biol* 48:1219–1231. doi:[10.1046/j.1365-2427.2003.01082.x](https://doi.org/10.1046/j.1365-2427.2003.01082.x)
- del Giorgio PA, Davis J (2003) Patterns in dissolved organic matter lability and consumption across aquatic ecosystems. In: Findlay S, Sinsabaugh RL (eds) *Aquatic ecosystems interactivity dissolved organic matter*. Academic Press, Elsevier, pp 400–424
- Döll P, Fiedler K, Zhang J (2009) Global-scale analysis of river flow alterations due to water withdrawals and reservoirs. *Hydrol Earth Syst Sci* 13:2413–2432. doi:[10.5194/hess-13-2413-2009](https://doi.org/10.5194/hess-13-2413-2009)
- Duarte CM, Prairie YT (2005) Prevalence of heterotrophy and atmospheric CO₂ emissions from aquatic ecosystems. *Ecosystems* 8:862–870. doi:[10.1007/s10021-005-0177-4](https://doi.org/10.1007/s10021-005-0177-4)
- Fellman JB, Hood E, Edwards RT, D'Amore DV (2009) Changes in the concentration, biodegradability, and fluorescent properties of dissolved organic matter during stormflows in coastal temperate watersheds. *J Geophys Res* 114:G01021. doi:[10.1029/2008JG000790](https://doi.org/10.1029/2008JG000790)
- Fellman JB, Hood E, Spencer RGM (2010) Fluorescence spectroscopy opens new windows into dissolved organic matter dynamics in freshwater ecosystems: a review. *Limnol Oceanogr* 55:2452–2462. doi:[10.4319/lo.2010.55.6.2452](https://doi.org/10.4319/lo.2010.55.6.2452)
- Fellman JB, Dogramaci S, Skrzypek G et al (2011) Hydrologic control of dissolved organic matter biogeochemistry in pools of a subtropical dryland river. *Water Resour Res*. doi:[10.1029/2010WR010275](https://doi.org/10.1029/2010WR010275)
- Fellman JB, Spencer RGM, Raymond PA et al (2014) Dissolved organic carbon biolability decreases along with its modernization in fluvial networks in an ancient landscape. *Ecology* 95:2622–2632
- Fellman JB, Hood E, Raymond PA et al (2015) Evidence for the assimilation of ancient glacier organic carbon in a proglacial stream food web. *Limnol Oceanogr* 60:1118–1128. doi:[10.1002/lno.10088](https://doi.org/10.1002/lno.10088)
- Francis C, Sheldon F (2002) River Red Gum (*Eucalyptus camaldulensis* Dehnh.) organic matter as a carbon source in the lower Darling River, Australia. *Hydrobiologia* 481:113–124
- Gasith A, Resh VH (1999) Streams in Mediterranean climate regions: abiotic influences and biotic responses to predictable seasonal events. *Annu Rev Ecol Syst* 30:51–81. doi:[10.1146/annurev.ecolsys.30.1.51](https://doi.org/10.1146/annurev.ecolsys.30.1.51)
- Green SA, Blough NV (1994) Optical absorption and fluorescence properties of chromophoric dissolved organic matter in natural waters. *Limnol Oceanogr* 39:1903–1916
- Guillemette F, del Giorgio PA (2011) Reconstructing the various facets of dissolved organic carbon bioavailability in freshwater ecosystems. *Limnol Oceanogr* 56:734–748. doi:[10.4319/lo.2011.56.2.0734](https://doi.org/10.4319/lo.2011.56.2.0734)
- Her N, Amy G, Foss D et al (2002) Optimization of method for detecting and characterizing NOM by HPLC-size exclusion chromatography with UV and on-line DOC detection. *Environ Sci Technol* 36:1069–1076. doi:[10.1021/es015505j](https://doi.org/10.1021/es015505j)
- Hornberger GM, Kelly MG (1975) Atmospheric reaeration in a river using productivity analysis. *J Environ Eng Div* 101:729–737
- Huguet A, Vacher L, Relexans S et al (2009) Properties of fluorescent dissolved organic matter in the Gironde Estuary. *Org Geochem* 40:706–719. doi:[10.1016/j.orggeochem.2009.03.002](https://doi.org/10.1016/j.orggeochem.2009.03.002)
- Korak JA, Dotson AD, Summers RS, Rosario-Ortiz FL (2014) Critical analysis of commonly used fluorescence metrics to characterize dissolved organic matter. *Water Res* 49:327–338. doi:[10.1016/j.watres.2013.11.025](https://doi.org/10.1016/j.watres.2013.11.025)
- Kothawala DN, Murphy KR, Stedmon CA et al (2013) Inner filter correction of dissolved organic matter fluorescence. *Limnol Oceanogr Methods* 11:616–630. doi:[10.4319/lom.2013.11.616](https://doi.org/10.4319/lom.2013.11.616)
- Lake PS (2003) Ecological effects of perturbation by drought in flowing waters. *Freshw Biol* 48:1161–1172. doi:[10.1046/j.1365-2427.2003.01086.x](https://doi.org/10.1046/j.1365-2427.2003.01086.x)
- Lakowicz JR (2006) *Principles of fluorescence spectroscopy*. Springer, New York
- Lawaetz AJ, Stedmon CA (2009) Fluorescence intensity calibration using the Raman scatter peak of water. *Appl Spectrosc* 63:936–940
- Lewis W, Wallace D (1998) Program Developed for CO₂ System Calculations. ORNL/CDIAC-105
- McArthur MD, Richardson JS (2002) Microbial utilization of dissolved organic carbon leached from riparian litterfall. *Can J Fish Aquat Sci* 59:1668–1676. doi:[10.1139/f02-135](https://doi.org/10.1139/f02-135)
- McCallister SL, Del Giorgio PA (2012) Evidence for the respiration of ancient terrestrial organic C in northern temperate lakes and streams. *Proc Natl Acad Sci U S A* 109:16963–16968. doi:[10.1073/pnas.1207305109](https://doi.org/10.1073/pnas.1207305109)
- Meyer JL, Wallace JB, Eggert SL (1998) Leaf litter as a source of dissolved organic carbon in streams. *Ecosystems* 1:240–249
- Mosley LM (2015) Drought impacts on the water quality of freshwater systems; review and integration. *Earth Sci Rev* 140:203–214. doi:[10.1016/j.earscirev.2014.11.010](https://doi.org/10.1016/j.earscirev.2014.11.010)
- Neal C, Neal M, Warrington A et al (1992) Stable hydrogen and oxygen isotope studies of rainfall and streamwaters for two contrasting holm oak areas of Catalonia, northeastern Spain. *J Hydrol* 140:163–178. doi:[10.1016/0022-1694\(92\)90239-R](https://doi.org/10.1016/0022-1694(92)90239-R)
- Neff JC, Finlay JC, Zimov SA et al (2006) Seasonal changes in the age and structure of dissolved organic carbon in Siberian rivers and streams. *Geophys Res Lett* 33:L23401. doi:[10.1029/2006GL028222](https://doi.org/10.1029/2006GL028222)
- Parlanti E, Wörz K, Geoffroy L, Lamotte M (2000) Dissolved organic matter fluorescence spectroscopy as a tool to estimate biological activity in a coastal zone submitted to anthropogenic inputs. *Org Geochem* 31:1765–1781. doi:[10.1016/S0146-6380\(00\)00124-8](https://doi.org/10.1016/S0146-6380(00)00124-8)
- R Core Team (2015) R: a language and environment for statistical computing. R Foundation for Statistical Computing, Vienna
- Raymond PA, Bauer JE (2001) Riverine export of aged terrestrial organic matter to the North Atlantic Ocean. *Nature* 409:497–500

- Romaní AM, Vázquez E, Butturini A (2006) Microbial availability and size fractionation of dissolved organic carbon after drought in an intermittent stream: biogeochemical link across the Stream-Riparian interface. *Microb Ecol* 52:501–512. doi:[10.2307/25153403](https://doi.org/10.2307/25153403)
- Sabater S, Tockner K (2010) Effects of hydrologic alterations on the ecological quality of river ecosystems. In: Sabater S, Barceló D (eds) *Water scarcity Mediterr*. Springer, Berlin, pp 15–39
- Sachse A, Henrion R, Gelbrecht J, Steinberg CEW (2005) Classification of dissolved organic carbon (DOC) in river systems: influence of catchment characteristics and autochthonous processes. *Org Geochem* 36:923–935. doi:[10.1016/j.orggeochem.2004.12.008](https://doi.org/10.1016/j.orggeochem.2004.12.008)
- Siebers AR, Pettit NE, Skrzypek G et al (2015) Alluvial ground water influences dissolved organic matter biogeochemistry of pools within intermittent dryland streams. *Freshw Biol*. doi:[10.1111/fwb.12656](https://doi.org/10.1111/fwb.12656)
- Šimek K, Comerma M, García J-C et al (2010) The Effect of River water circulation on the distribution and functioning of reservoir microbial communities as determined by a relative distance approach. *Ecosystems* 14:1–14. doi:[10.1007/s10021-010-9388-4](https://doi.org/10.1007/s10021-010-9388-4)
- Singer GA, Fasching C, Wilhelm L et al (2012) Biogeochemically diverse organic matter in Alpine glaciers and its downstream fate. *Nat Geosci* 5:710–714
- Sinsabaugh RL, Foreman CM (2003) Integrating dissolved organic matter metabolism and microbial diversity: an overview of conceptual models. In: Findlay S, Sinsabaugh RL (eds) *Aquatic ecosystems interactivity dissolved organic matter*. Elsevier, Academic Press, pp 426–454
- Stuiver M, Polach HA (1977) Discussion: reporting of ^{14}C data. *Radiocarbon* 19:355–363
- Tittel J, Büttner O, Freier K et al (2013) The age of terrestrial carbon export and rainfall intensity in a temperate river headwater system. *Biogeochemistry* 115:53–63
- Trumbore S, Schiff S (1992) Sources and transformation of dissolved organic carbon in the Harp Lake forested catchment: the role of soils. *Radiocarbon* 34:626–635
- Vázquez E, Amalfitano S, Fazi S, Butturini A (2011) Dissolved organic matter composition in a fragmented Mediterranean fluvial system under severe drought conditions. *Biogeochemistry* 102:59–72. doi:[10.1007/s10533-010-9421-x](https://doi.org/10.1007/s10533-010-9421-x)
- Vázquez E, Ejarque E, Ylla I et al (2015) Impact of drying/rewetting cycles on the bioavailability of dissolved organic matter molecular-weight fractions in a Mediterranean stream. *Freshw Sci* 34:263–275. doi:[10.1086/679616](https://doi.org/10.1086/679616)
- Volk CJ, Volk CB, Kaplan LA (1997) Chemical composition of biodegradable dissolved organic matter in streamwater. *Limnol Oceanogr* 42:39–44
- von Schiller D, Acuña V, Graeber D et al (2011) Contraction, fragmentation and expansion dynamics determine nutrient availability in a Mediterranean forest stream. *Aquat Sci* 73:485–497. doi:[10.1007/s00027-011-0195-6](https://doi.org/10.1007/s00027-011-0195-6)
- von Schiller D, Graeber D, Ribot M et al (2015) Hydrological transitions drive dissolved organic matter quantity and composition in a temporary Mediterranean stream. *Biogeochemistry* 123:429–446. doi:[10.1007/s10533-015-0077-4](https://doi.org/10.1007/s10533-015-0077-4)
- Weishaar JL, Aiken GR, Bergamaschi BA et al (2003) Evaluation of specific ultraviolet absorbance as an indicator of the chemical composition and reactivity of dissolved organic carbon. *Environ Sci Technol* 37:4702–4708. doi:[10.1021/es030360x](https://doi.org/10.1021/es030360x)
- Wetzel RG (1983) *Limnology*, second edition. Saunders
- Ylla I, Sanpera-Calbet I, Muñoz I et al (2011) Organic matter characteristics in a Mediterranean stream through amino acid composition: changes driven by intermittency. *Aquat Sci* 73:523–535. doi:[10.1007/s00027-011-0211-x](https://doi.org/10.1007/s00027-011-0211-x)
- Zhang J, Quay PD, Wilbur DO (1995) Carbon isotope fractionation during gas-water exchange and dissolution of CO_2 . *Geochim Cosmochim Acta* 59:107–114. doi:[10.1016/0016-7037\(95\)91550-D](https://doi.org/10.1016/0016-7037(95)91550-D)
- Zhang X, Marcé R, Armengol J, Tauler R (2014) Distribution of dissolved organic matter in freshwaters using excitation emission fluorescence and multivariate curve resolution. *Chemosphere* 111:120–128
- Zsolnay A, Baigar E, Jimenez M et al (1999) Differentiating with fluorescence spectroscopy the sources of dissolved organic matter in soils subjected to drying. *Chemosphere* 38:45–50. doi:[10.1016/S0045-6535\(98\)00166-0](https://doi.org/10.1016/S0045-6535(98)00166-0)